Dynamic force microscopic study of a triblock copolymer with the AFM non contact resonant mode

F. Dubourg[1], G. Couturier[1], J.P. Aimé[1*], S. Marsaudon[1], P. Leclère[2], R. Lazzaroni[2], J. Salardenne[1], R. Boisgard[1]

[1] CPMOH, Université de Bordeaux I
351, Cours de la Libération, F-33405 Talence Cedex (France)

[2] Service de Chimie des Matériaux Nouveaux,
Centre de Recherche en Science des Matériaux Polymères (CRESMAP)
Université de Mons-Hainaut, Place du Parc 20, B-7000 Mons (Belgium)

Abstract: We present an experimental study of a triblock copolymer with the AFM non contact resonant mode. This dynamic force microscope allows the attractive tip surface interaction to be finely tuned by varying the shift of the resonance frequency. The triblock copolymer chosen exhibits a periodic structure of lamellae with different mechanical properties. Height and dissipation images are recorded at different resonance frequency shifts. The dissipation images show the influence both of the strength of the attractive interaction and of the mechanical properties onto the contrast. In addition a comparative study between Tapping and dissipation images is performed. reverse contrast observed is explained as a direct consequence of the intrinsic mechanical properties of each lamella.

I Introduction.

In latter years, dynamic force microscopy (DFM) has been proven to image soft material and to image surfaces of semi-conductors and insulators at the atomic scale [1-8]. Several modes of DFM measurements make use of the change of oscillation characteristics of the cantilever due to tip-surface interactions. Either the change of the oscillation amplitude and of the phase at fixed excitation frequency or the shift of the resonance frequency can be used to control the tip-sample distance. The first mode is usually called Tapping and the second non-contact atomic force microscopy (NC–AFM). For small tip-sample distances, say less than the nanometer, the tip-sample interaction can be large enough so that a non-linear dynamical behavior of the oscillating system occurs [9-16].

The high sensitivity of the NC-AFM mode is due to the distortion of the top of the resonance peak that leads to an abrupt variation of the resonance frequency as a function of

 CCC 1022-1360/00/$ 17.50+.50/0

tiny variations of the attractive tip-sample interaction. The oscillation amplitude is kept constant in a NC-AFM experiment. When the tip approaches the surface, in general the oscillation amplitude decreases. An electronic loop is required to keep the oscillation constant by varying the excitation amplitude a_{exc}. We can thus record two types of information, one is the resonance frequency shift connected to the attractive tip sample interaction, and the second is the variation of a_{exc} related to the loss of energy of the oscillator. Experiments show a change of the damping coefficient that depends abruptly of the tip-sample distance [7, 17-21]. Since the tip does not touch the sample, question rises on the physical origin of the increase of the loss of energy. A few recent works have been specially dedicated to the study of the microlever energy loss in NC-AFM. Reference 18 gives a detailed description of the electronic loop that keeps the oscillation amplitude constant, a rather important point to check as change of the shape of the resonance peak can induce a decrease of the oscillation amplitude. Reference 19 describes the origin of the additional dissipation as a consequence of a Brownian motion while reference 20 suggests that a process of Joule dissipation induce an additional loss of energy. The latter experiments were performed on conducting material with a conducting tip [20]. A Δ^{-4} power law is obtained, where Δ is the closest tip-sample distance. In references 7 and 17, the experimental works demonstrated the ability of local energy dissipation measurements on silicium [7] and on films of NaCl on Cu(111) in UHV of producing images with a contrast at the nm-scale [17]. In reference [21], the local deformation of the sample under the action of the oscillating tip is considered as being the leading term to explain the physical origin of the additional dissipation. Comparison between the NC-AFM results performed on a graphite surface and theoretical predictions provide an excellent agreement [21].

In the present paper we focus on the recording of dissipation image measured on a soft material. The model system used is a triblock copolymer exhibiting a well-defined periodic lamellar structure.

II Experimental conditions.

The triblock copolymer is made of PMMA-b-polyButylacrylate-b-PMMA sequences with molecular weight 10-50-10 kDalton respectively. The morphology of this copolymer has been extensively described elsewhere [2]. This triblock copolymer is a model system for the present study because of its ability to produce well-defined periodic lamellar structure with different mechanical properties [2, 22]. Thin films of copolymers (typically 500 nm- thick)

were prepared by solvent casting from a 2 mg/mL. Then, the copolymer was annealed at 140°C under secondary vacuum (10^{-7} Torr) for 48 hours.

The experiments were performed with a hybrid NC-AFM made of a Digital Instrument head driven by a controller NSE and the Omicron electronic system. Both non-contact and Tapping modes can be performed with the same equipment. The cantilever is a TESP-NCL from Nanosensors. The results were obtained in a vacuum chamber with a primary vacuum (20 mBar). The oscillating loop of the Omicron electronic tracks the cantilever resonance frequence. Usually, the phase shifter is adjusted in order that the frequency of the loop is equal to the resonance frequency $f_0=\omega_0/2\pi$ of the cantilever for a infinite tip-surface distance D. As D decreases, the frequency of the loop is no longer equal to f_0, consequently the frequency loop is no more equal to the new resonance frequency of the cantilever. However, for large values of the quality factor Q, or small damping coefficient β_0, because the phase varies very abruptly near the resonance frequency, the frequency loop is very close to that of the new resonance frequency. In these conditions, it has been shown that the damping signal D_{amp} is directly proportional to the damping coefficient of the oscillating cantilever [21].

In the present work, the resonance frequency is ν_0 = 179873 Hz, the quality factor Q = 2000 and the oscillation amplitude A = 10 nm. Typical resonance frequency shift and change of D_{amp} to maintain the resonant oscillation amplitude constant are displayed in Figures 1.

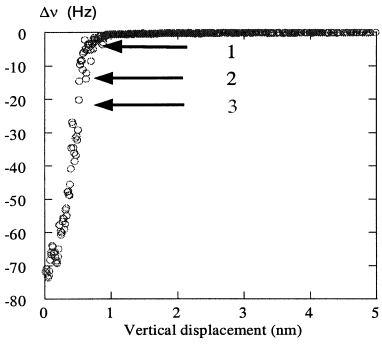

Figure 1a: Resonance frequency shift as a function of the vertical displacement. Arrows indicate the set-points used to record the image displayed in Figure 3.

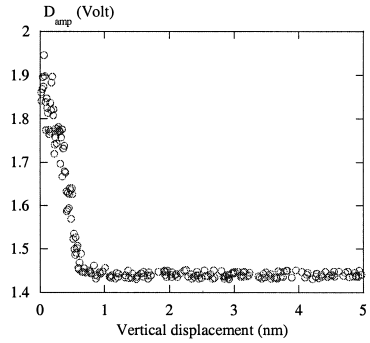

Figure 1b: Variation of the gain (D_{amp}) proportional to a_{exc} as a function of the vertical displacement.

The electronic loop that keeps the oscillation amplitude constant has a large time constant, about the ms. Thus, to obtain an image in which the measured quantities correspond

to steady state values of the oscillator requires to scan the surface at a low frequency. Typically, images of size 400 nm x 400 nm are recorded at scanning frequencies 0.1 Hz-0.05 Hz. In particular, such a slow scanning rate is needed for dissipation image recording the variation of a_{exc}.

Typical height and dissipation images are shown in Figures 2. The height image (figure 2a) shows a smooth (or featureless) surface, indicating that, within the nanometer, there is no height variation due to the topography. This first result was already deduced from an experimental study performed in the Tapping mode [22]. The dissipation image (Figure 2b), simultaneously recorded, gives the corresponding variations of the excitation amplitude required to keep constant the oscillation resonant amplitude at any X,Y location in the image. The difference is striking, while no contrast is observed with the height image, a well-defined structure exhibiting lamella morphology is shown in the dissipation image. As a first step, the observed contrast is readily understood by considering the simple relationship between the oscillation amplitude A and the excitation amplitude a_{exc} : $A = Q\ a_{exc}$, where Q is the quality factor, with $Q = \omega_0/\beta_T$. β_T is the sum of the intrinsic damping coefficient β_0 and an effective one β_{eq}, the magnitude of which being a function of the tip sample distance and of the mechanical properties of the material [21] (see also Appendix).

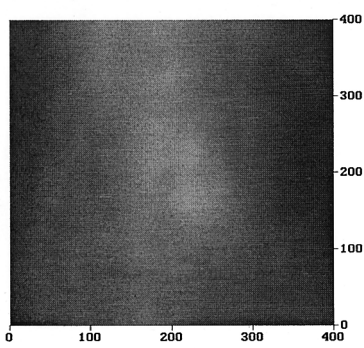

Figure 2a: Height image obtained at a given resonance frequency shift. Contrast 0-10 nm.

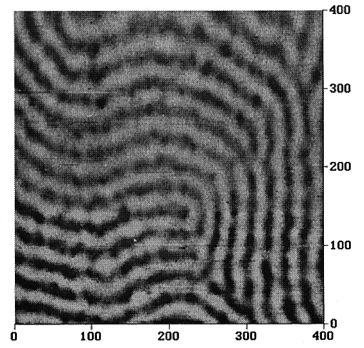

Figure 2b: Recorded simultaneous Dissipation image.

Figure 3 shows a dissipation image recorded at three different shifts of the resonance frequency. The image shows a direct correlation between the magnitude of the shift and the contrast of the image.

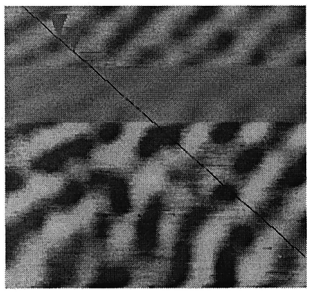

Fig. 3: Dissipated image recorded at three different resonance frequency shift (see figure 1a).

The contrast is strongly enhanced when the resonance frequency shift is increased (bottom of the image). The highest contrast correspond to the highest resonance frequency shift (arrows noted 3 in Figure 1a). Since the increase of the resonance frequency shift leads to an increase of the tip surface interaction [11-14], this image indicates that larger is the interaction between the tip and the sample, larger is the energy dissipated by the cantilever.

As previously described, our hybrid AFM allows the two dynamic modes to be used: Tapping and NC-AFM. Figure 4 shows a comparison between Tapping and NC-AFM images which have been sequentially recorded. Tapping height image and NC-dissipation image exhibit an exact reverse contrast, the bright (dark) lamella observed in Tapping become dark (bright) in NC-AFM.

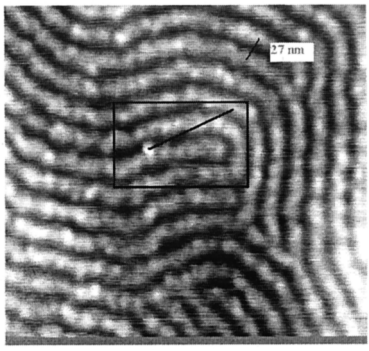

Figure 4a: Tapping height image. The lamella period is 27 nm

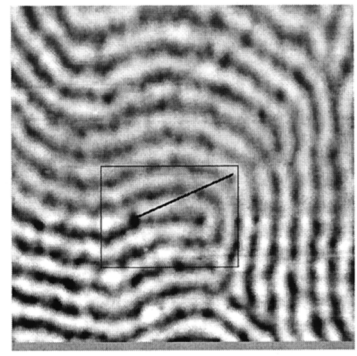

Figure 4b: NC dissipation image recorded at the same X,Y location.

III Discussion.

Non contact dissipation or enhancement of dissipation induced due to the attractive tip sample interaction has been recently discussed in detail [21] (see also Appendix). The basic idea is the following: for a tip of radius of ten nanometers, the Van der Waals interaction leads to an attractive force varying in the domain of nanoNewton or less. This domain of force is large enough to induce a small viscoelastic displacement of the sample without the need of touching the surface with the tip [23]. For a perfect elastic displacement, the sample response

is instantaneous and there is no additional work dissipated. If any relaxation processes occur, there is a time delay between the action of the tip and the sample response, thus part of the work performed by the oscillating nanotip onto the surface is not recovered by the oscillator.

A simple mathematical approach is used to derive analytical expressions describing change of the oscillator's damping coefficient as a function of the tip sample distance. For time relaxation of the viscoelastic material shorter than that of the period, equations A6a and A6b give two asymptotic regimes. From these two equations several behaviors can be predicted. (i)- the increase of the damping coefficient varies as the square of the strength of the attractive interaction, therefore smaller is the closest distance between the tip and the sample larger is the work dissipated into the sample; (ii)– the time during which the tip is closed to the sample, noted residence time τ_{res}, is a function of the magnitude of the oscillation amplitude. Since the period of the oscillator is the same whatever the oscillation amplitude, large amplitudes lead to smaller residence times and weaker attractive forces; (iii)– the exponents of the power law dependence as a function of the closest distance $\Delta = D - A$ and of the amplitude predict that varying one of these two parameters should lead to sizeable difference on dissipation image; (iv)– the amount of dissipation is a function of the mechanical susceptibility, equations A6 predict that the softest material must exhibit a larger dissipation.

These equations predict that for a plane surface containing heterogeneous mechanical properties, the height image can show a flat structure while the dissipation image will exhibit a contrast. This is what is observed in figures 2. Moreover, one expects an increase of the dissipation when the closest tip-sample distance Δ is reduced. This is what is illustrated in the Figure 3 for which, stronger is the attractive interaction between the tip and the surface, more pronounced is the contrast between the two types of lamellae. Figure 3 provides a direct estimation of the sensitivity obtained by this dynamic force mode. The energy dissipated per period is given by $E_{diss} = \pi k A^2/Q$, when the tip is far from the surface the quality factor is 2000, thus with an amplitude A = 10 nm and a spring constant $k \approx 40$ Nm^{-1}, the dissipated energy is $E_{diss} \approx 6.3\ 10^{-18}$ J corresponding to a damping signal of 1.4 V. When the image is recorded, the lowest difference detected corresponds to the smallest resonance frequency shift (arrow noted as 1 in Figure 1a). The contrast is about 5 mV, giving a detectable variation of the dissipated energy of $\Delta E_{diss} \approx 2\ 10^{-20}$ J. Since the sensitivity of the measurement is proportional to the quality factor, measurements done in secondary vacuum, leading to an oscillator quality factor of 10000 or more, will lead to a sensitivity of about k_BT.

The last point concerns the respective contribution of the hard and soft compounds. This can be checked with the help of a direct comparison between Tapping height images and

NC-Dissipation images. In general for Tapping mode (but also for NC-AFM) one can demonstrate [19, 26] and unambiguously show experimentally [22] that the image contrast can be a pure mechanical one. For example, it has been shown that the bright (dark) part of the Tapping height images and phase images is due to glassy (elastomer) domains [22]. This is a direct consequence of the fact that the vertical displacement of the piezo-actuator is a function of the sample contact stiffness. Since the tip indentation depth is larger for the elastomer lamellae, for a flat surface the soft lamella appears lower. On the contrary, equations A6 predict the opposite for NC-dissipation images, which is in very good agreement with the images shown (figures 4).

The mathematical development uses a simple description of the sample mechanical response. The amount of energy dissipated in the sample is controlled by the magnitude of a spring constant and a damping coefficient. Evaluation of the dissipated energy can be done by considering the motion of the monomer units under the action of the attractive interaction. In that case, one has to estimate the characteristic time involved. From the Einstein relation one gets the relationship between the monomeric friction coefficient and the diffusion coefficient:

$$D = \frac{k_B T}{\gamma} \qquad (1)$$

By using the definition of the diffusion coefficient, the time required to move through a monomer unit length λ is given by:

$$\tau = \frac{\lambda^2}{D} = \frac{\lambda^2 \gamma}{k_B T} \qquad (2)$$

The second step is to estimate the velocity of the molecules during the action of the tip, that is during the residence time τ_{res}. One gets:

$$v_m \sim \frac{\lambda}{\tau_{res}} \qquad (3)$$

Using expression 2 and 3, the energy dissipated by period is given by:

$$E_{dis} \sim n_m f_{dis} v_m \tau_{res} = n_m \gamma v_m^2 \tau_{res} = n_m k_B T \frac{\tau}{\tau_{res}} \qquad (4)$$

Where n_m is the number of monomer units involved in the process. A typical amount of additional dissipated energy is 100 k_BT, giving the relation $n_m\tau \sim 100\tau_{res}$. Thus, with n_m in the order of hundred monomer units, the characteristic relaxation time is $\tau \sim 10^{-7}$ s, which is a very reasonable value for polymer in glassy and elastomeric state [24].

While the general trends are quite well verified, other contributions to the dissipated energy can take place. For example, instability within the sample producing hysteresis loop like stick-slip phenomena can happen. Also one cannot avoid the possibility of small jumps of polymer touching the tip during a very short time, thus giving an additional contribution through hysteresis of adhesion [25].

Conclusion

The present work is an attempt to probe nanomechanical properties with the Non Contact resonant mode of a dynamic force microscope. The main goal is to access sample properties by taking advantage of the attractive tip sample interaction in order to weaken the perturbation on a soft material. The Non Contact resonant mode is used because the strength of the attractive interaction can be easily controlled by varying the resonant frequency shift of the oscillating cantilever. A triblock copolymer is used as a model system. The copolymer exhibits well defined periodic lamellar morphology with a period of 27 nm presenting specific mechanical properties for each lamella. Height and dissipation images are simultaneously recorded. While the height image shows a perfect flat surface, the dissipation image reveals structure directly related to the different mechanical properties. The dissipation contrast is shown to be modulated by varying the resonant frequency shift. This experimental result is in good agreement with the prediction of a simple model describing the additional amount of cantilever dissipation as a consequence of the attractive interaction between the tip and the copolymer. Comparison with Tapping images is also performed showing reverse contrast as predicted. The present work shows that nanomechanical properties can be measured uniquely by taking advantage of the attractive tip sample interaction.

Appendix

The time during which the tip is close to the surface is called the residence time, following the approach given in reference 17, one can consider an average tip-sample distance Δ at proximity of the surface such that the residence time is given by $\tau_{res} \approx \frac{T}{\pi}\sqrt{\frac{2\Delta}{A}}$ with the period $T = 2\pi/\omega_0$. Therefore, the action of the oscillating tip can be described as a rectangular periodic function of width τ_{res} and height $F_{ext} = HR/6\Delta^2$ [17]. For fast relaxation times of the protuberance β^{-1}, with $\beta >> \omega_0/2\pi$, the action of the oscillating tip can described as a pulse of width τ_{res} so that an integration can be used instead of the Fourier series. The dissipated energy due to the attractive interaction between the tip and the sample is:

$$\langle E_{diss} \rangle_T = \int_0^\infty \omega \chi''(\omega) |f_\omega|^2 \frac{d\omega}{\pi} \quad (A1)$$

With the Fourier coefficient $f_\omega = 2F_{ext}\left(\sin(\omega\frac{\tau_{res}}{2})/\omega\right)$ at the frequency ω and $\chi''(\omega)$ the imaginary part of the generalised susceptibility $\chi = \chi' + i\chi''$ with $\chi''(\omega)$ given by:

$$\chi''(\omega) = \frac{\omega\gamma}{k^2 + \gamma^2\omega^2} \quad (A2)$$

Equation 3 expresses the situation of a surface with a viscoelastic mechanical response that can be represented with a spring constant k (Nm^{-1}) and a damping factor γ (kg s^{-1}) in parallel. For example, we may consider that the locality of the coupling between the oscillating tip and the surface is described by a local elastic response of the surface with a stiffness k which is coupled to a surrounding medium of mass M with an intrinsic molecular relaxation time $\tau_m = \beta^{-1}$ thus a damping term $\gamma = M\beta$. Equation 2 leads to the result:

$$\langle E_{diss} \rangle_T = \frac{(HR)^2}{36\Delta^4}\frac{1}{k}\left(1 - \exp\left(-\frac{\tau_{res}\, k}{\gamma}\right)\right) \quad (A3)$$

Two asymptotic regimes, which are determined by the values of the ratio $\tau_{res}k/\gamma$, are extracted from equation 4. The asymptotic regimes correspond to two limiting cases of the sample mechanical response.

For $\tau_{res}k/\gamma << 1$ equation 4 can be by replaced by:

$$\langle E_{diss}\rangle_T \approx \frac{(HR)^2}{36\Delta^4}\frac{\tau_{res}}{\gamma}$$

$$\approx \frac{(HR)^2}{18\Delta^{7/2}}\frac{1}{A^{1/2}}\frac{\sqrt{2}}{\gamma\,\omega_0} \qquad \text{(A4a)}$$

where τ_{res} has been substituted by $\frac{2}{\omega_0}\sqrt{\frac{2\Delta}{A}}$

while for $\tau_{res}k/\gamma >> 1$ one gets:

$$\langle E_{diss}\rangle_T \approx \frac{(HR)^2}{36\,\Delta^4}\frac{1}{k} \qquad \text{(A4b)}$$

Equation 5b means that the average dissipation energy per pulse is mainly governed by the magnitude of the local stiffness, while equation 5a exhibits explicitly the viscous process. Equation 5a would be more suitable for material having a dominant friction behavior and, or dissipating processes due to diffusion motion while equation 5b is more likely to describe hard surface behavior with phonon assisted dissipation.

We now have to express that the oscillator looses this energy during a period. The simplest way to describe the loss of energy is to use an equivalent damping coefficient β_{eq} that becomes a function of the closest tip-sample distance Δ. The energy dissipated during a period is given by:

$$\langle E_{diss}\rangle_T = m\,\pi\,\beta_{eq}(\Delta)\,\omega_0\,A^2 = k_c\,\pi\,\beta_{eq}(\Delta)\frac{A^2}{\omega_0} \qquad \text{(A5)}$$

Where k_c is the cantilever stiffness. Combining equations (A4) and (A5) gives an expression of the equivalent damping coefficient :

$$\beta_{eq}(\Delta) \approx \left(\frac{\sqrt{2}}{\pi\,k_c}\frac{(HR)^2}{18\,\gamma}\frac{1}{\Delta^{7/2}}\frac{1}{A^{5/2}}\right) \qquad \text{(A6a)}$$

$$\beta_{eq}(\Delta) \approx \left(\frac{\omega_0}{\pi\,k_c}\frac{(HR)^2}{36\,k}\frac{1}{\Delta^4}\frac{1}{A^2}\right) \qquad \text{(A6b)}$$

Reference

[1] Stocker, W.; Beckmann, J.; Stadler, R.; Rabe, J.P. *Macromolecules*, **29**, 7502 (1996).

[2] Leclère, Ph.; Lazzaroni, R.; Brédas, J.L.; Yu, J.M.; Dubois, Ph.; Jérôme, R. *Langmuir* 12**,** 4317 (1996); Leclère, Ph. ; Moineau, G. ; Minet, M. ; Dubois, Ph. ; Jérôme, R. Brédas, J.L. ; Lazzaroni R. *Langmuir*, **15**, 3915 (1999). A. Rasmont, Ph. Leclère, C. Doneux, G. Lambin, J.D. Tong, R. Jérôme, J.L. Brédas, R. Lazzaroni, Colloids and Surfaces B: Biointerfaces, *in press.*

[3] Magonov, S.N.; Elings, V.; Wangbo, M.H. *Surf. Sci.* **389**, 201 (1997).

[4] F. J. Giessibl, Sciences **267**, 68 (1995)

[5] Y. Sugarawa, M. Otha, H. Ueyama, S. Morita Sciences **270**, 1646 (1995)

[6] S. Kitamura, M. Iwatsuki, Jpn J. Appl. Phys. **35,** L668 (1996)

[7] M. Bammerlin et al Probe Microscopy **1** 3 (1997)

[8] A. Schwarz, W. Allers, U.D. Schwarz, R. Wiesendanger, Appl. Surf. Sci. **140**, 293 (1999)

[9] Gleyzes P.,Kuo P.K.,Boccara A.C., Appl. Phys. Lett. **58,** 25 (1991)

[10] B. Anczykowski, D. Krüger, H. Fuchs, Phys. Rev. B , **53**, 15485, (1996).

[11] F. J. Giessibl Phys. Rev. B **56**, 16010 (1997).

[12] R. Boisgard, D. Michel, J. P. Aimé Surf. Science, **401**, 199 (1998). J.P. Aimé, R. Boisgard, G. Couturier, L. Nony Phys. Rev. Let. **82**, 3388 (1999).

[13] Holscher, U.D. Schwarz, R. Wiesendanger, Appl. Surf. Sci. **140**, 344 (1999)

[14] N. Sasaki, M. Tsukada, , Appl. Surf. Sci. **140**, 339 (1999)

[15] Tamayo, J.; Garcia, R. *Appl. Phys. Lett.* **73**, 2926 (1998); Tamayo, J; Garcia, R. *Appl. Phys. Lett.* **71**, 2394 (1997).

[16] Nony, L.; Boisgard R.; Aimé, J. P. *J. Chem. Phys.* **111**, 1615 (1999).

[17] R. Bennewitz, A.S. Foster, L.N. Kantorovich, M. Bammerlin, C. Loppacher, S. Schär, M. Guggisberg, E. Meyer, A. L. Shluger, Phys. Rev. B, to be published (2000).

[18] B. Gotsmann, C. Seidel, B. Anczykowski and H. Fuchs, PRB **60**, 11051 (1999).

[19] M. Gauthier, M. Tsukada Phys. Rev. B **60**, 11716 (1999).

[20] L. Dorofeyev, H. Fuchs, G. Wenning, B. Gotsmann Phys. Rev. Let. **83**, 2402 (1999).

[21] G. Couturier, J.P. Aimé, J. Sarladenne, A. Gourdon, S. Gauthier, J. of Appl. Phys. A, to be published; G. Couturier, J.P. Aimé, J. Sarladenne, R. Boisgard submitted.

[22]. S. Kopp-Marsaudon, Ph. Leclère, F. Dubourg, R. Lazzaroni, J.P. Aimé, Langmuir, **16**, No 22, 8432 (2000).

[23] J.P. Aimé, D. Michel, R. Boisgard, L. Nony Phys. Rev. B **59**, 2407 (1999).

[24] J.D. Ferry, Viscoelastic Properties of Polymers (Wiley, New York, 1970). E. Kramer and L. Berger, Adv. Polym. Sci. 91 (1990).

[25] B. Gostmann, H. Fuchs, to be published, J. Appl. Phys. A

[26] F. Dubourg, J.P. Aimé, S. Marsaudon, L. Nony, R. Boisgard ; F. Dubourg, S. Marsaudon, P. Leclère, J.P. Aimé, R. Lazzaroni ; in preparation.